

Nitrate ion detection in aerosols using morphology-dependent stimulated Raman scattering

Pamela M. Aker, Jian-Xiang Zhang, and William Nichols

Citation: *The Journal of Chemical Physics* **110**, 2202 (1999); doi: 10.1063/1.477832

View online: <http://dx.doi.org/10.1063/1.477832>

View Table of Contents: <http://scitation.aip.org/content/aip/journal/jcp/110/4?ver=pdfcov>

Published by the [AIP Publishing](#)

Articles you may be interested in

[Standoff explosives trace detection and imaging by selective stimulated Raman scattering](#)

Appl. Phys. Lett. **103**, 061119 (2013); 10.1063/1.4817248

[Coherent control of stimulated Raman scattering using chirped laser pulses](#)

Phys. Plasmas **8**, 3531 (2001); 10.1063/1.1382820

[Far-ultraviolet resonance Raman spectroscopy of nitrate ion in solution](#)

J. Chem. Phys. **113**, 6760 (2000); 10.1063/1.1310615

[Comment on "Morphology-dependent stimulated Raman scattering imaging" \[*J. Chem. Phys.* 105, 7276 \(1996\)\]](#)

J. Chem. Phys. **109**, 9199 (1998); 10.1063/1.477474

[Morphology-dependent stimulated Raman scattering imaging. I. Theoretical aspects](#)

J. Chem. Phys. **105**, 7268 (1996); 10.1063/1.472587



Nitrate ion detection in aerosols using morphology-dependent stimulated Raman scattering

Pamela M. Aker,^{a)} Jian-Xiang Zhang, and William Nichols

Department of Chemistry, University of Pittsburgh, Pittsburgh, Pennsylvania 15260

(Received 29 June 1998; accepted 23 October 1998)

A nitrate ion concentration of 5×10^{-5} M has been detected in ~ 180 μm diam aqueous aerosols using morphology-dependent stimulated Raman scattering (MDSRS). This low concentration was detected by allowing the droplet size to be tuned during an experiment. Comparison of the experimental results with the MDSRS gain equation shows that it may be possible to detect concentrations a factor of ten lower. © 1999 American Institute of Physics.
[S0021-9606(99)02304-1]

INTRODUCTION

The recent interest in determining the impact that heterogeneous chemistry has on global atmospheric chemical balance has catalyzed the development of new spectroscopic methods that are capable of characterizing airborne particles. Several novel spectroscopies have surfaced. These include particle analysis by laser mass spectroscopy (PALMS),¹ cavity enhanced Raman spectroscopy (CERS),² and morphology-dependent stimulated Raman scattering (MDSRS).^{3,4}

PALMS is principally used to determine fundamental aerosol chemical makeup. While the data generated from PALMS field measurements is extremely valuable, the destructive sampling methodology precludes one from obtaining specific information on individual chemical speciation within the aerosol and corresponding absolute concentration. CERS and MDSRS spectroscopies are capable of providing the latter information, however these spectroscopies have not been used as field measurement tools principally because their detection sensitivities are thought to be too low. For example, MDSRS and CERS measurements on sulfate aerosols have reported detection limits of only 0.15 and 0.001 M, respectively.^{2,3} Recent two-color MDSRS measurements on sulfate aerosols report higher signal levels than seen in the one-color experiments, suggesting an improved sensitivity, but spectra could be generated only for 0.2 M concentration.⁵ The gain equation for the one-color MDSRS process shows, however, that significantly higher sensitivity can be achieved.³ Analyte concentrations around 3×10^{-5} M should be detectable if the species' Raman cross sections are on the order of magnitude of that seen for sulfate ($10 \times 10^{-30} \text{ cm}^2 \text{ mol}^{-1} \text{ sr}^{-1}$). We show here that these small concentrations can indeed be detected. This result suggests that MDSRS spectroscopy field measurements may provide information that both complements and extends that obtained from PALMS studies.

MDSRS is a nonlinear spectroscopy that uses the set of "macroscopic" natural electromagnetic modes of oscillation characteristic of micron-sized axisymmetric particles to en-

hance Raman scattering from molecules contained within the particle. The modes of oscillation are commonly called morphology-dependent resonances (MDRs) because their spatial and spectral positions are determined by particle size, shape, and refractive index.

MDRs can enhance Raman scattering from molecules located inside a particle *via* two independent mechanisms. First, if the wavelength of an external excitation source is in resonance with an MDR, external light will couple efficiently into the "input" MDR mode volume, and remain trapped there for the lifetime of the cavity mode. Because the trapped light continues to circulate within the particle, the net effect is one of optical path lengthening. For example, if an MDR has a lifetime, $\tau=20$ ns, then the path length becomes $l = \tau c/m = 4.5$ m (here c is the speed of light, and m is the refractive index of the material comprising the particle). The MDR lifetime is given by the mode Q factor, i.e., $\tau = Q/\omega$, where ω is the angular frequency ($\omega = 2\pi c/\lambda$).

The second mechanism involves a separate MDR which is commonly called an "output" or Stokes MDR. If the output MDR's wavelength is in resonance with the Stokes (or anti-Stokes) transitions of the molecules that comprise the particle, molecules found in the output mode volume will undergo stimulated Raman scattering, provided of course that pump light is also present in the output mode volume.

The MDSRS signal is the largest and therefore the optical detection is the most sensitive when these two mechanisms operate simultaneously. This requires not only that the particle be sized such that both the input and output MDRs match the requisite pump and Stokes shifted wavelengths, but also that input and output mode volumes overlap, as much as possible, in space. These criteria can be satisfied provided that either the particle size or the excitation wavelength can be tuned during the course of an MDSRS experiment.

We illustrate this here by considering the case where the particle size can be tuned. Specifically we discuss detecting trace amounts of nitrate in ~ 180 μm diam water droplets using a 532 nm excitation source that has a 0.15 cm^{-1} line-width (used here in the experiment). We first present results of theoretical calculations that demonstrate how changing

^{a)}Electronic mail: pamaker@vms.cis.pitt.edu

droplet size changes both the ability to tune into an input MDR and the overlap that occurs between the input and output MDRs. Next we outline the experimental apparatus and procedure that was used to detect nitrate ion in droplets and present MDSRS spectra generated for a nitrate ion concentration of 5×10^{-5} M. Finally, a comparison of the experimental results with that predicted by the MDSRS gain equation shows that slight modifications to the experiment may allow the theoretical detection limit of 5×10^{-6} M to be reached.

EFFECT OF DROPLET SIZE ON NITRATE ION MDSRS SIGNAL GENERATION

We will examine the possibility of detecting MDSRS from trace amounts of nitrate ion contained in ~ 180 μm diam water droplets using a 532 nm excitation source. The first thing we need to consider is the strengths, widths, and polarization of the different nitrate ion spontaneous Raman bands. Solution phase studies commonly focus on two modes; the ν_1 symmetric stretch at ~ 1050 cm^{-1} Raman shift and the ν_4 deformation at the ~ 720 cm^{-1} Raman shift.⁶ The ν_1 band has a fairly large spontaneous Raman cross section, measured at 10×10^{-30} $\text{cm}^2 \text{mol}^{-1} \text{sr}^{-1}$,⁷ but its bandwidth is narrow, ~ 11.5 cm^{-1} .⁸ The ν_4 mode cross section has not been measured but in linear Raman spectra this band's intensity is approximately a factor of two smaller than that of the ν_1 band. The ν_4 bandwidth is quite large, however, ~ 35 cm^{-1} .^{9,10}

Since our experimental apparatus allows us to generate droplets with a size stability of 1 part in 10^5 ,^{11,12} we consider what happens when droplets are tuned to four different sizes, these being 180.000, 179.960, 178.471, and 179.992 μm diameter. The large particle Lorenz-Mie algorithm of Schiller *et al.*¹³ is used to calculate the input and Stokes MDR wavelengths. In these calculations it is assumed that dilute nitrate solutions have a refractive index identical to that of water, i.e., $m = 1.33384$.¹⁴ It is also assumed that the incident beam is *s* polarized, hence only input MDRs of transverse electric (TE) polarization can be excited.^{12,13} Raman scattering can occur from both transverse magnetic (TM) or TE output Stokes modes in the case of the 720 cm^{-1} ν_4 transition because it is depolarized ($\rho = 0.7$).¹⁰ Appreciable inelastic scattering will only occur from TE Stokes modes in the case of the ν_1 transition, however, because this band is strongly polarized ($\rho = 0.05$).¹⁰ The polarization selection rules have an interesting effect on an MDSRS experiment. While the ν_4 Raman cross section is smaller than that for ν_1 , there is a higher chance of observing the former transition because it has a larger probability that there is good spatial overlap between the input and output MDRs.

We first consider exciting a 180.000 ± 0.002 μm diam droplet (the error in size is the experimental uncertainty). Table I shows the various input and Stokes output MDRs associated with this droplet. As can be seen, there are three TE input modes that can be excited: $n = 1262$, $l = 16$; $n = 1196$, $l = 27$; and $n = 1398$, $l = 1$. The relative role that these MDRs take when the MDSRS signal is generated from the nitrate contained in the droplet is different, however. First, as we have previously shown, the experimental illumi-

TABLE I. Input and Stokes nitrate MDRs for a 180,000 μm diam droplet.

	Input	n	l	$\lambda(\text{nm})$	$b_{n,\text{obs}}^2/b_{n,\text{res}}^2$
	TE	1262	16	532.006	0.37
	TE	1196	27	531.999	0.91
	TE	1398	1	531.993	0.33

Stokes ν_1	n	l	$\lambda(\text{nm})$	Raman shift (cm^{-1})	Overlap with 1196
TE	1149	22	563.517	1051.3	0.004
TE	1199	14	563.514	1051.2	$< 10^{-5}$
TE	1121	16	563.514	1051.2	0.194
TE	1132	25	563.512	1050.7	0.247
TE	1252	7	563.488	1050.4	$< 10^{-5}$
TE	1213	12	563.482	1050.2	$< 10^{-5}$
TE	1167	19	563.457	1049.4	$< 10^{-5}$
TE	1206	13	563.457	1049.4	$< 10^{-5}$
TE	1155	21	563.453	1049.3	$< 10^{-5}$
TE	1304	2	563.434	1048.7	$< 10^{-5}$
TE	1161	20	563.432	1048.6	0.001
TE	1261	6	563.427	1048.5	$< 10^{-5}$
TE	1186	16	563.398	1047.5	$< 10^{-5}$
TE	1095	32	563.396	1047.5	$< 10^{-5}$
TE	1228	10	563.378	1046.9	$< 10^{-5}$
TE	1080	35	563.363	1046.4	$< 10^{-5}$
TE	1090	33	563.362	1046.4	$< 10^{-5}$
TE	1085	34	563.351	1046.1	$< 10^{-5}$
TE	1116	28	563.345	1045.9	$< 10^{-5}$

Stokes ν_4	n	l	$\lambda(\text{nm})$	Raman shift (cm^{-1})	Overlap with 1196
TE	1155	25	553.467	729.1	0.097
TM	1149	26	553.442	728.3	0.661
TM	1155	25	553.249	722.0	0.104
TE	1150	26	553.229	721.3	0.550

nation geometry dictates the amount of light I_{MDR} that can be coupled into a specific MDR.^{11,12} Second, I_{MDR} is also determined by the mode Mie plane wave internal coefficient b_n^2 , which in turn depends on the degree of resonance match between the MDR and the excitation source, i.e., $b_{n,\text{obs}}^2 = b_{n,\text{res}}^2 \Delta\lambda^2 / [(\lambda_{\text{in}} - \lambda_{\text{MDR}})^2 + \Delta\lambda^2]$, where λ_{in} and λ_{MDR} are the input and MDR wavelengths and $\Delta\lambda^2$ is the experimental linewidth which is ± 0.005 nm in our experiment.^{11,12} The $b_{n,\text{obs}}^2/b_{n,\text{res}}^2$ ratios for the $n = 1262$, 1196, and 1398 MDRs are 0.37, 0.91, and 0.33, respectively; hence we need only consider signal generated from the $n = 1196$, $l = 27$ mode since the gain in the other two modes will be too small for stimulated Raman scattering to occur. In the following we assume that if an input MDR has a $b_{n,\text{obs}}^2/b_{n,\text{res}}^2$ ratio less than 0.5 it will not contribute significantly to MDSRS signal generation from dilute nitrate solutions.

Table I shows that there are 19 TE modes that lie underneath the nitrate ν_1 spontaneous Raman band. Not all of these modes will participate in generating stimulated Raman signal however. This is because most of the Stokes output MDRs do not overlap well with the TE $n = 1196$, $l = 27$ input MDR. The exact degree of overlap can be determined by integrating $O(r, \theta, \phi) = \iint \psi_{\text{Stokes}}(r, \theta, \phi) \psi_{\text{input}}(r, \theta, \phi) dr d\theta d\phi$, where the individual MDR wave functions are given by the standard vector spherical harmonics.¹⁵ Previous studies have shown that the

overlap in the θ and ϕ dimensions can be represented by fairly simple functions, i.e., $O(\theta) = [(2n_{\text{Stokes}} + 1)/(2n_{\text{input}} + 1)]^{1/2}$, and $O(\phi) = 1$ (for equatorial illumination geometry which is what we use).¹¹ Unfortunately a simple function is not available for determining the degree of overlap in the radial dimension. It therefore becomes necessary to numerically integrate the spherical Bessel functions that describe the MDR electric fields in this dimension, i.e., $O(r) = \int j_{n,\text{Stokes}}(mk_{\text{Stokes}}r)j_{n,\text{input}}(mk_{\text{input}}r)dr / \int j_{n,\text{input}}(mk_{\text{input}}r)j_{n,\text{input}}(mk_{\text{input}}r)dr$, where $k = 2\pi/\lambda$. We used MATHEMATICA 3.0 and a 133 MHz personal computer to do these calculations. The resulting exact overlap factors, $O(r, \theta, \phi) = O(r)O(\theta)O(\phi)$ are listed in the far right column of Table I.

The results of the formal overlap calculations show that only two Stokes ν_1 nitrate MDRs, specifically the TE $n = 1149$, $l = 22$ and TE $n = 1132$, $l = 25$ modes have non-negligible overlap factors (defined as >0.1), and even then these values are small: 0.194 and 0.247, respectively. Thus only these modes will participate in nitrate MDSRS signal generation in a 180.000 μm diam droplet. This result is a bit “disappointing” if one considers the time spent performing the overlap calculations, which was approximately 1.5 h for each input/output MDR combination. Computation time can be shortened, however, if a means by which to estimate which specific input/output MDR combinations would have non-negligible overlap factors was available. The calculations we have performed here show that the overlap functions become significant only when the peak of the Stokes mode radial electric field closely coincides with the peak of the input mode’s radial electric field. We note here that this does not necessarily mean that there is an exact match between the input and outmode mode l values. We have previously shown that TE modes peak at $r = \lambda/2\pi m\{0.750 \exp[0.3443 \ln(n)] + n + 0.5\}$, and TM modes at $r = \lambda/2\pi m\{0.606 \exp[0.3646 \ln(n)] + n + 0.5\}$.¹¹ To determine the mode combinations that have significant overlap then, for TE input coupled to TE Stokes output, one need only solve for n_{Stokes} using

$$0.750 \exp[0.3443 \ln(n_{\text{Stokes}})] + n_{\text{Stokes}} + 0.5 = \lambda_{\text{input}}/\lambda_{\text{Stokes}}\{0.75 \exp[0.3443 \ln(n_{\text{input}})] + n_{\text{input}} + 0.5\}, \quad (1)$$

and

$$0.606 \exp[0.3646 \ln(n_{\text{Stokes}})] + n_{\text{Stokes}} + 0.5 = \lambda_{\text{input}}/\lambda_{\text{Stokes}}\{0.75 \exp[0.3443 \ln(n_{\text{input}})] + n_{\text{input}} + 0.5\}, \quad (2)$$

for TE input coupled to TM Stokes output.

To illustrate the effectiveness of this “shortcut” method, let us reconsider the ν_1 nitrate Stokes MDRs listed in Table I. Knowing that the input MDR has $\lambda = 532.0$ nm and $n = 1196$, and that the output MDR has $\lambda \sim 563.4$ nm, the right hand side equation becomes equal to 1137.94. Overlap will therefore be a maximum when $n_{\text{Stokes}} = 1129$. The data in Table I show that overlap is non-negligible (i.e., >0.1) when

TABLE II. Input MDRs for a 179.960 μm diam droplet.

Input	n	l	$\lambda(\text{nm})$	$b_{n,\text{obs}}^2/b_{n,\text{res}}^2$
TM	1397	1	532.006	0
TM	1320	8	532.005	0
TM	1179	30	531.983	0

n_{Stokes} is within ± 10 of this maximum, hence in this case formal overlap calculations need only be done for those Stokes modes with $n = 1119$ –1139.

We used the “shortcut” method to hone in on the TE and TM nitrate ν_4 Stokes modes that would couple well with the input TE $n = 1196$, $l = 27$ mode of a 180.000 μm diam droplet. This band has $\lambda_{\text{Stokes}} = 553.2$ nm. The above equation shows that overlap will be maximum for TE and TM Stokes modes when $n_{\text{max}} \sim 1150$. Table I shows that the overlap is quite large (0.661 and 0.550) for the TM $n = 1149$, $l = 26$ and TE $n = 1150$, $l = 26$ MDRs, respectively, while the overlap factors become negligible when $\Delta n = n_{\text{max}} - n > 5$.

The overlap factors presented in Table I show that it would be difficult to detect small quantities of nitrate in a 180.000 μm diam droplet. While two and four Stokes output modes lie underneath the ν_1 and ν_4 nitrate bands, respectively, these modes have relatively small overlap factors. The MDSRS nitrate ion detection limit can be reached only when the overlap is close to 1. This situation may be achieved by tuning the droplet diameter to other values.

We consider next a 179.960 μm diam droplet. The input modes associated with this particular sized system are listed in Table II. Here it can be seen that while three modes are in resonance with our excitation source laser (a Nd:YAG laser), none of these could be excited if the incident source were s polarized, as it is in our particular experiment. This is because all of the modes have TM polarization. Hence MDSRS signal would not be seen from any species, whatsoever, contained in this droplet.

Tuning the droplet size to 178.471 μm diameter provides a better situation. In this case Table III shows that there

TABLE III. Input and Stokes nitrate MDRs for a 178.471 μm diam droplet.

Input	n	l	$\lambda(\text{nm})$	$b_{n,\text{obs}}^2/b_{n,\text{res}}^2$	
TE	1278	12	532.027	0.030	
TE	1219	21	532.013	0.128	
TE	1386	1	532.000	1.000	
TE	1264	14	531.9631	0.016	
Stokes ν_1	n	l	$\lambda(\text{nm})$	Raman shift (cm^{-1})	Overlap with 1386
TE	1280	3	563.550	1052.3	$< 10^{-5}$
TE	1308	1	563.419	1048.2	1.000
TE	1121	2	563.319	1045.1	$< 10^{-5}$
Stokes ν_4	n	l	$\lambda(\text{nm})$	Raman shift (cm^{-1})	Overlap with 1386
TM	1331	1	553.506	730.3	0.940
TE	1332	1	553.363	725.7	0.970
TM	1332	1	553.094	716.9	0.940
TE	1317	2	553.229	721.3	$< 10^{-5}$

TABLE IV. Input and Stokes nitrate MDRs for a 179.992 μm diam droplet.

	Input	n	l	$\lambda(\text{nm})$	$b_{n,\text{obs}}^2/b_{n,\text{res}}^2$
	TM	1184	29	532.003	0
	TE	1236	20	532.000	1.000
	TM	1163	33	531.991	0
Stokes ν_1	n	l	$\lambda(\text{nm})$	Raman shift (cm^{-1})	Overlap with 1236
TE	1179	17	563.405	1047.8	0.010
TE	1143	23	563.371	1046.7	$<10^{-5}$
Stokes ν_4	n	l	$\lambda(\text{nm})$	Raman shift (cm^{-1})	Overlap with 1236
TM	1189	19	553.463	728.9	0.626
TM	1183	20	553.426	727.7	0.603
TE	1190	19	553.271	722.7	0.466
TE	1178	21	553.236	721.5	$<10^{-5}$
TE	1184	20	553.231	721.4	0.810
TM	1190	19	553.039	715.1	0.466
TM	1184	20	553.002	713.9	0.774

are four input modes available to be excited: the TE $n = 1278$, $l = 12$; $n = 1219$, $l = 21$; $n = 1386$, $l = 1$; and $n = 1264$, $l = 14$. The $b_{n,\text{obs}}^2/b_{n,\text{res}}^2$ ratios for these modes are, however, 0.03, 0.128, 1.0, and 0.016, respectively, hence the MDSRS signal will only be seen from Stokes nitrate modes that overlap with the $n = 1386$, $l = 1$ input MDR. Table III shows that there are three TE Stokes modes that lie underneath the ν_1 Raman band and four that lie under the ν_4 band. One of the modes associated with the former transition, specifically the TE $n = 1308$, $l = 1$ has a large overlap factor with the input $n = 1386$, $l = 1$ MDR. In this case $O(r, \theta, \phi) = 0.97$, hence this particular droplet diameter would maximize the nitrate ν_1 MDSRS detection sensitivity. We also note that this particular sized droplet would also give a signal from the ν_4 nitrate band. Specifically, three modes; TM $n = 1331$, $l = 1$; TE $n = 1332$, $l = 1$; and TM $n = 1332$, $l = 1$, have large overlap factors, 0.94, 0.97, and 0.94, respectively.

Other droplet diameters can also give rise to dilute nitrate MDSRS. Table IV shows the input and Stokes output modes for a 179.992 μm diam droplet. Here it can be seen that there is one input MDR, specifically the TE $n = 1236$, $l = 20$. There are two and seven modes that lie underneath the ν_1 and ν_4 Stokes bands, but the MDSRS signal would only be seen from the TE $n = 1184$, $l = 20$ ν_4 Stokes mode as this is the only MDR that overlaps significantly with the input MDR.

The data contained in Tables I, III, and IV illustrate the necessity of being able to tune the particle size (or conversely the incident wavelength) if low concentrations of dopant species are to be detected in an MDSRS experiment. Different diameter droplets have different sets of input MDRs available to be excited. Similarly, the associated sets of output Stokes modes vary in identity, along with their respective overlap factors. We note that in the case where large diameter particles are probed, the size (or wavelength) variability does not have to be large—tuning the diameter over a 5 μm range is more than sufficient to maximize the

input/output MDR overlap factors for a species with a fairly narrow Raman bandwidth (10 cm^{-1}).

EXPERIMENTAL APPARATUS AND PROCEDURE

Since our MDSRS spectrometer has been described in detail in previous publications we provide only a brief description of the experiment here.^{3,4,16} The system basically consists of a Nd:YAG (Continuum NY 61-10) operating on the second harmonic. The incident laser beam is focused off one side of a droplet stream that is generated using a home-built vibrating orifice aerosol generator (VOAG). The Stokes shifted MDSRS light is collected at right angles to the incident beam, directed into a triple monochromator (SPEX), dispersed and detected with a diode array (Princeton Applied Research OMA III). The throughput of the collection optics assembly is estimated to be 2.4×10^{-3} .

Incident laser powers of 2.5 mJ/pulse were used, and the light was focused to a 90 μm spot diameter using a 15 cm focal length lens. Droplets between 175 and 185 μm diameter were generated using a 100 μm diam orifice in the VOAG, vibrating frequencies between 25 and 35 kHz, and a liquid flow rate $\sim 0.1 \text{ cm}^3 \text{ s}^{-1}$. Droplets generated using the VOAG are charged.¹² Since charge modifies the MDR Q factors and thus reduces the sensitivity limit (see below), it was eliminated by passing the droplet stream through a counter charging assembly that has been described previously.¹² Sodium nitrate (Fisher Scientific, certified ACS grade) was used as the nitrate ion source.

Nitrate ion MDSRS intensity was monitored as a function of droplet size by tuning VOAG frequency in increments of $\sim 0.1 \text{ Hz}$. When the signal was maximum, spectra were collected by coadding spectra from 30 individual laser shots. The spectra were then treated with a three point smoothing routine to reduce the noise.

RESULTS

Nitrate ion spectra were recorded for concentrations ranging between 3×10^{-3} and $5 \times 10^{-5} \text{ M}$. In general it was found that it was easier to generate signal from the ν_4 band as compared to the ν_1 band. This is an expected result since the ν_4 transition has a larger bandwidth. The MDSRS spectra collected for the ν_1 and ν_4 transitions at a nitrate concentration of $5 \times 10^{-5} \text{ M}$ are shown in Figs. 1 and 2, respectively. The signal for the ν_1 transition is quite small—the ~ 15 count peak seen at 1048 cm^{-1} Raman shift is just barely discernable above the noise, and the signal is narrow—the band has a full width half maximum (FWHM) of 15 cm^{-1} which corresponds to the resolution of the monochromator (0.6 nm). The large background count in this spectrum is primarily due to unwanted 532 nm scattered light. Figure 2 shows that the ν_4 MDSRS signal bandwidth is large, $\sim 40 \text{ cm}^{-1}$ FWHM. This is an expected result. But what is surprising, however, is the ν_4 MDSRS intensity—at ~ 250 counts it is about ten times larger than that for the ν_1 band. This is not an expected result since the linear Raman nitrate spectra show that the latter signal is about twice as intense as the former.

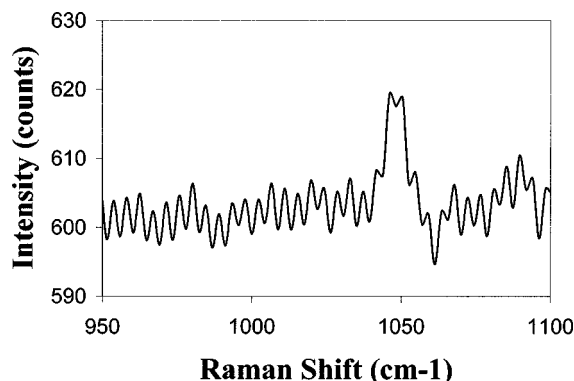


FIG. 1. MDSRS signal from the nitrate ion ν_1 band. The concentration is 5×10^{-5} M.

DISCUSSION

We now look to the MDSRS gain equation to estimate the nitrate ion detection limit. We have previously shown that the nonlinear gain is³

$$I_{\text{MDSRS}} = \exp[I_g A N (d\sigma/d\Omega) O(r, \theta, \phi) Q_s Q_g f_{\text{sca}}]. \quad (3)$$

Here $A = 16\pi^3 c^3 / h \omega_g^2 \omega_s^3 m_s^2$, with g and s referring to the input and Stokes waves, N is the species number density (molecule cm^{-3}), $(d\sigma/d\Omega)$ is the molecular Raman cross section ($\text{cm}^2 \text{molecule}^{-1} \text{sr}^{-1}$), $O(r, \theta, \phi)$ is the spatial overlap factor discussed above, Q_g and Q_s are the input and Stokes output MDR Q factors, and f_{sca} is the ratio of the probabilities for scattering of the stimulated Raman light from the green mode and absorption into the red mode. $f_{\text{sca}} = f_n^2 / d_n^2$, where f_n is the Mie scattering coefficient which is $f_n^2 = (2n_g + 1)a_n^2 = (2n_g + 1)$, since $a_n = 1$ because red light is scattered with unit efficiency from a green mode.¹⁷ d_n^2 is the Mie absorption coefficient, which is related to the Stokes mode Q factor via $\ln d_n^2 = -0.50119 \ln(x_s/Q_s) + 0.70784$, where x is the droplet size parameter, $x_s = 2\pi a/\lambda_s$ and a is the droplet radius.¹¹

In the above equation, I_g is the total intensity in the input MDR volume. We have previously shown that the angle averaged electric field intensity is a function of the illumination geometry.^{11,12} Thus for excitation of an input TE mode,

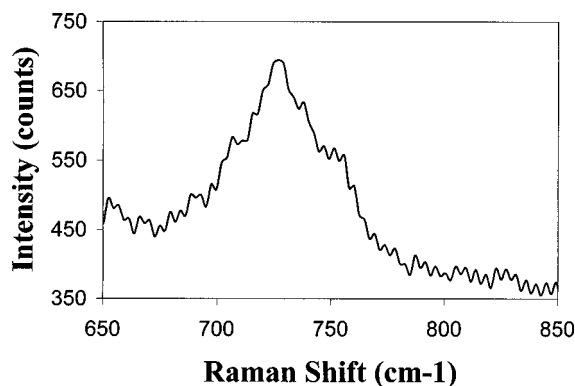


FIG. 2. MDSRS signal from the nitrate ion ν_4 band. The concentration is 5×10^{-5} M.

$$I_g = \int I_g(r) dr = (E_0^2/2)(2n_g + 1)B_n^2 d_n^2 \int j_n^2(mkr) dr, \quad (4)$$

where E_0 is the incident beam electric field magnitude and B_n is the weighted beam coefficient that describes the TE component of the localized incident Gaussian laser beam which is focused at the droplet.⁷ Assuming, for illustration purposes, that an incident 2.5 mJ/pulse beam is focused to a 90 μm spot diameter at a distance 120 μm from the center of a 178.471 μm diam droplet that has an $n = 1386$ input mode, the above equation shows that $I_g = 3.97 \text{ GW cm}^{-2}$.

Using the data on the wavelength dependence of the water refractive index (at 25 $^\circ\text{C}$),¹⁴ the A terms for the nitrate ν_1 and ν_4 Raman transitions are calculated to be 2.42×10^{-11} and $2.29 \times 10^{-11} \text{ cm}^3 \text{s J}^{-1}$, respectively. Data on the wavelength dependence of water absorption can also be used to determine the Q_g and Q_s factors. We have previously shown that in the case of nonionic liquid systems, MDR Q factors can be determined using

$$1/Q_{\text{exp},t} = 1/Q_{\text{abs}} + 1/Q_{\text{disp}} + 1/Q_{\text{reorient}}, \quad (5)$$

where $Q_{\text{abs}} = m/2k_{\text{im}}$, and Q_{disp} and Q_{reorient} are 8×10^{11} and 1.3×10^9 for water.¹¹ When ions are present in the system, however, further Q factor degradation occurs because ion migration causes the MDR electric fields to decay more rapidly than if no ions were present. An extra term must now be added to the right hand side of Eq. (5), specifically $1/Q_{\text{ion}}$, where $Q_{\text{ion}} = \omega t_{\text{ion}}$. The ion relaxation time $t_{\text{ion}} = \epsilon/\kappa$, where $\epsilon = D\epsilon_0$, where D is the dielectric constant, ϵ_0 is the vacuum permittivity, and κ is the conductivity of the medium ($\Omega^{-1} \text{cm}^{-1}$).¹⁸ The κ of a solution is related to the ion concentration through $\kappa = \Lambda_m c$, where Λ_m is the molar conductivity and c is the molar concentration.¹⁹ A 5×10^{-5} M sodium nitrate solution has $t_{\text{ion}} = 9.6 \times 10^{-7} \text{ s}$. Using the k_{im} values for water¹⁴ and the t_{ion} value just given, it is calculated that a 5×10^{-5} M solution has $Q_g = 2.8 \times 10^8$, $Q_{\nu_1} = 1.9 \times 10^8$, and $Q_{\nu_4} = 2.3 \times 10^8$.

We would like to point out here that Eq. (5) is valid only in cases where the particle being excited has a homogeneous interior. Prior studies we have done on charged water aerosols show that there is some structuring of the water in the interface region.¹² Charged aerosols are therefore inhomogeneous. Theoretical studies on inhomogeneous systems (modeled as a refractive index gradient) show that MDR Q factors and spectral line positions change with inhomogeneity magnitude,^{20–28} and preliminary measurements we have made show that Q factors degrade when water droplets are charged. For experiments geared at determining MDSRS detection limits it is therefore important to ensure that the sample is not charged, as we have done, in order to maximize the Q factors and therefore the sensitivity.

When the appropriate numbers are substituted into the MDSRS gain equation and it is assumed that $O(r, \theta, \phi) = 0.97$, the maximum value seen in the theoretical calculations, the results show that the net gain for the 5×10^{-5} M ν_1 nitrate system is $G_{\text{MDSRS}} = 5.14$. The experimental signal count is related to the gain via

$$I_{\text{MDSRS}} = N T_{\text{exp}} \exp(G_{\text{MDSRS}}), \quad (6)$$

where N is the number of spectra collected and T_{exp} is the collection optics throughput, which we estimate to be 2.48×10^{-3} . With $N=30$, an MDSRS gain of 5.14 gives an experimental signal count of 13. This number is in excellent agreement with the experimentally measured 15 counts.

A factor of ten improvement in nitrate ion MDSRS detection sensitivity can be achieved if a higher incident power is used. Prior studies in our lab show that droplets of the size we use can be illuminated with incident beam intensities ranging up to 9 GW cm^{-2} before plasma induced explosions occur.¹² Substitution of this energy into Eq. (3) shows that $G_{\text{MDSRS}}=1$ for a nitrate ion concentration of $5 \times 10^{-6} \text{ M}$. It may be possible to further decrease the concentration and still generate the nitrate MDSRS signal by shifting the incident source wavelength into the ultraviolet (UV). This is because the nitrate spontaneous Raman cross section increases with decreasing wavelength.⁷ However, it is not known if powers up to 9 GW cm^{-2} can be used because the plasma-induced explosion threshold is also wavelength dependent. The lower limit of MDSRS nitrate detection is therefore estimated to be $5 \times 10^{-6} \text{ M}$.

If it is assumed that the spontaneous Raman cross section for the ν_4 band is one half that for the ν_1 band, a $5 \times 10^{-5} \text{ M}$ nitrate solution would have $G_{\text{MDSRS}}=2.47$ and an experimental signal count $I_{\text{MDSRS}}=1$. This value does not agree with the 250 counts seen in the experiment. One possible source of the discrepancy is our estimate of the spontaneous Raman cross section—we may be using too low a value. However our estimate would have to be 3.3 times larger in order to give the experimentally observed $G_{\text{MDSRS}}=8.11$. It is unlikely that the linear Raman intensity measurements could be this far off.

The increase in the observed G_{MDSRS} over that predicted with the gain equation can be explained by considering the case where several input MDRs are simultaneously excited in the experiment. While the data in Tables I–IV show situations where only one input MDR can be excited, there is just as likely to be a case where several input MDRs are in resonance simultaneously with the excitation source.¹¹ In this case the net MDSRS gain is the sum of the gains for the individual input/output transitions, i.e., $G_{\text{MDSRS,net}} = G_{\text{MDSRS,1}} + G_{\text{MDSRS,2}} + \dots$, and therefore the experimental gain can become larger than that predicted by assuming only one transition is excited. We would like to point out that this situation is possible only for cases where experiments are done on large particles—i.e., the input MDR density becomes appreciably large only when the diameter is greater than $150 \mu\text{m}$ —and Raman transitions with large bandwidths are accessed.

CONCLUSION

By allowing either the particle size or the incident source wavelength to be tuned during an experiment, the MDSRS signal from small concentrations of Raman active species can be detected. Our experimental results show that the signal from a $5 \times 10^{-5} \text{ M}$ nitrate solution can be quite easily generated. The experimental intensities compare very well with the signal intensities predicted using the MDSRS gain equation. By increasing the incident source intensity the detection limit can be extended down to $5 \times 10^{-6} \text{ M}$.

ACKNOWLEDGMENT

This research was supported by the Office of Energy Science, Department of Energy, Division of Chemical Physics.

- ¹D. M. Murphy, D. S. Thomson, and A. M. Middlebrook, *Geophys. Res. Lett.* **24**, 3197 (1997).
- ²H.-B. Lin and A. J. Campillo, *Opt. Lett.* **20**, 1589 (1995).
- ³J.-X. Zhang and P. M. Aker, *J. Chem. Phys.* **99**, 9366 (1993).
- ⁴J.-X. Zhang and P. M. Aker, *J. Photochem. Photobiol., A* **80**, 381 (1994).
- ⁵L. Pasternack, J. W. Fleming, and J. Owrutsky, *J. Opt. Soc. Am. B* **13**, 1510 (1996).
- ⁶D. E. Irish and M. H. Brooker, in *Advances in Infrared and Raman Spectroscopy*, edited by R. J. H. Clark and R. E. Hester (Heyden, London, 1976), Vol. 2, Chap. 6.
- ⁷J. M. Dudik, C. R. Johnson, and S. A. Asher, *J. Chem. Phys.* **82**, 1732 (1985).
- ⁸P. M. Vollmar, *J. Chem. Phys.* **39**, 2236 (1963).
- ⁹D. E. Irish and A. R. Davis, *Can. J. Chem.* **46**, 943 (1968).
- ¹⁰A. R. Davis and C. Chong, *Inorg. Chem.* **11**, 1891 (1972).
- ¹¹S. Schiller, *Appl. Opt.* **32**, 2181 (1993).
- ¹²P. M. Aker, P. A. Moortgat, and J.-X. Zhang, *J. Chem. Phys.* **105**, 7268 (1996).
- ¹³J.-X. Zhang, P. A. Moortgat, and P. M. Aker, *J. Chem. Phys.* **105**, 7276 (1996).
- ¹⁴G. M. Hale and M. R. Querry, *Appl. Opt.* **12**, 555 (1973).
- ¹⁵P. W. Barber and S. C. Hill, in *Light Scattering by Particles: Computational Methods* (World Scientific, Singapore, 1990).
- ¹⁶J.-X. Zhang, D. Aiello, and P. M. Aker, *J. Phys. Chem.* **99**, 721 (1995).
- ¹⁷M. Kerker, *The Scattering of Light and Other Electromagnetic Radiation* (Academic, New York, 1969).
- ¹⁸J. A. Stratton, *Electromagnetic Theory* (McGraw-Hill, New York, 1941), p. 15.
- ¹⁹P. W. Atkins, *Physical Chemistry*, 5th ed. (Freeman, New York, 1994).
- ²⁰J. Lock, *Appl. Opt.* **29**, 3180 (1990).
- ²¹D. Chowdhury, S. Hill, and P. Barber, *J. Opt. Soc. Am. A* **8**, 1702 (1992).
- ²²L. Kai and P. Massoli, *Appl. Opt.* **33**, 501 (1994).
- ²³T. Kaiser, S. Lange, and G. Schweiger, *Appl. Opt.* **33**, 7789 (1994).
- ²⁴E. Khaled, S. Hill, and P. Barber, *Appl. Opt.* **33**, 3308 (1994).
- ²⁵K. Fuller, *Opt. Lett.* **19**, 1272 (1994).
- ²⁶S. Hill, H. Saleheen, and K. Fuller, *J. Opt. Soc. Am. A* **12**, 905 (1995).
- ²⁷F. Onofri, G. Grehan, and G. Gousbet, *Appl. Opt.* **34**, 7113 (1995).
- ²⁸R. Hightower and C. B. Richardson, *Appl. Opt.* **27**, 4850 (1988).